Local Stability of *Rhodobacter capsulatus* Cytochrome c_2 Probed by Solution Phase Hydrogen/Deuterium Exchange and Mass Spectrometry

Guilong Cheng and Vicki H. Wysocki*
Department of Chemistry, University of Arizona, Tucson, Arizona, USA

Michael A. Cusanovich
Department of Biochemistry and Molecular Biophysics, University of Arizona, Tucson, Arizona, USA

The hydrogen/deuterium exchange kinetics of *Rhodobacter capsulatus* cytochrome c_2 have been determined using mass spectrometry. As expected, the relative domain stability was generally similar to that of the cytochrome c_2 structural homolog, horse heart cytochrome *c*, but we were able to find evidence to support the presence of a second, small β-sheet not found in the horse cytochrome, which stabilizes a structural region dominated by Ω loops. Importantly, we find that the so-called hinge region, comprised of 15 amino acids, which include the methionine sixth heme ligand (M96), is destabilized on oxidation, and this destabilization is propagated to a portion of the second Ω loop, most likely through perturbation of two hydrogen bonds that couple these two domains in the three dimensional structure. The mutation of a lysine at position 93 to proline amplifies the destabilization observed on oxidation of the wild-type cytochrome c_2 and results in further destabilization observed in regions 52–60, 75–82, and 83–97. This suggests that hydrogen bond interactions involving two bound waters, the T94 hydroxyl, the front heme propionate and the Y75 hydroxyl, are significantly compromised upon mutation. In summary, these observations are consistent with the ~20-fold increase in the movement of the hinge away from the heme face in the oxidized cytochrome c_2 as determined by ligand binding kinetics. Thus, H/D exchange kinetics can be used to identify relatively subtle structural features and at least in some cases facilitate the understanding of the structural basis of the dynamic properties of proteins. (J Am Soc Mass Spectrom 2006, 17, 1518–1525) © 2006 American Society for Mass Spectrometry

A wide range of techniques have been developed to relate structure and function in proteins. In recent years, there has evolved an increasing interest in the dynamic properties of proteins, and in particular understanding the structure of functionally relevant conformations that are not necessarily identical with the time-averaged structure. Cytochrome *c* has been of particular interest since it exists in two states (oxidized and reduced) that have almost identical structures, but very different properties (e.g., stability to denaturation and susceptibility to proteolytic digestion). In elegant studies from the Englander laboratory [1–3], hydrogen-deuterium (H/D) exchange as determined by NMR has been used to characterize the stability of cytochrome *c* domains. Figure 1a shows the five domains that can be resolved. These results are consistent with the native structure with the blue regions (N- and C-terminal helices) folding first, stabilizing the green regions (Ω loop and 60's helix) that fold next, then the yellow (Ω loop) and red (so-called hinge, see below) regions (see the Discussion section for more details) [3]. Thus, a folding pathway can be described, that is consistent with thermodynamic, kinetic, and structural information. A limitation of the NMR approach has been the need for relatively large amounts of material, hence constraining the ability to apply this technique to site-directed mutants or proteins that are available in limited quantities. As a consequence, the application of proteolytic fragmentation followed by mass spectrometry to measure localized amide hydrogen/deuterium exchange rates has been developed [4–6]. This approach yields conclusions consistent with the NMR H/D exchange studies, and requires relatively small amounts of material (1000-fold less).

Published online July 26, 2006

Address reprint requests to Professor M. A. Cusanovich, Department of Biochemistry and Molecular Biophysics, University of Arizona, 1041 E. Lowell St., Tucson, AZ 85721, USA. E-mail: cusanovi@u.arizona.edu

* Department of Biochemistry and Molecular Biophysics, University of Arizona, Tuscon, Arizona.

1044-0305/06/$32.00
doi:10.1016/j.jasms.2006.04.028

Received March 1, 2006
Revised April 25, 2006
Accepted April 26, 2006

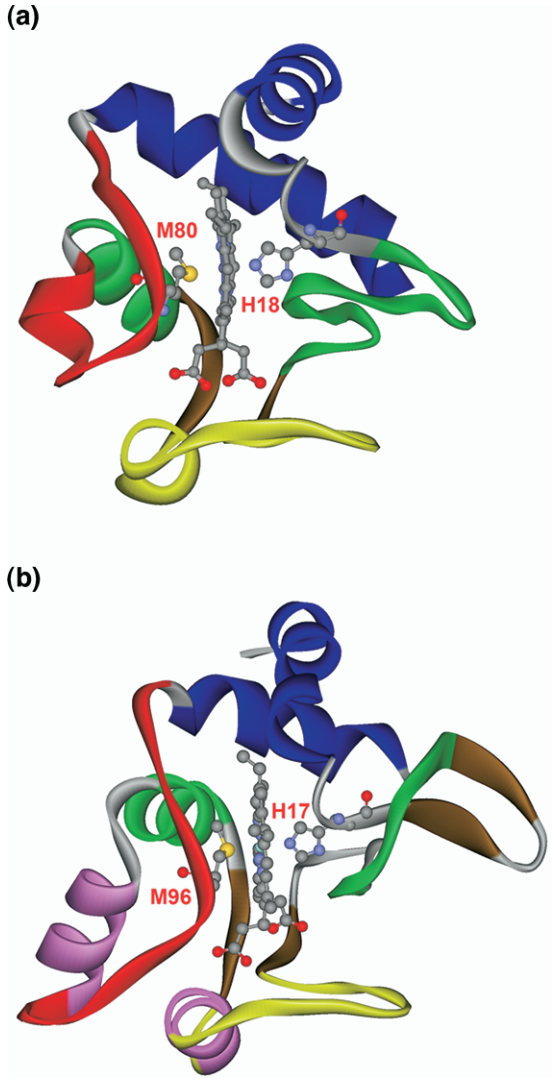

Figure 1. Cytochrome structures. (**a**) Horse heart cytochrome *c*, colored-coded according to Englander's five "foldons" [3]. The hinge region is in red, the helix regions in blue and green, Ω loops in yellow or green, and apparent regions of β-sheet in brown. (**b**) *Rhodobacter capsulatus* cytochrome c_2. Color coding is as in (**a**), based upon structural homology except for two helices that are in purple, and not clearly defined in horse heart cytochrome *c*.

We have focused on bacterial cytochrome c_2 from *Rhodobacter capsulatus*, which is a structural homolog of cytochrome *c* [7], but has quite distinct properties and is a subfamily of the class I *c*-type cytochromes [8]. Cytochrome c_2 functions as an electron carrier between the cytochrome b/c_1 complex and cytochrome oxidase (aerobic growth) or photosynthetic reaction centers (anaerobic growth in the light) in photosynthetic bacteria. It is larger than cytochrome *c* (116 versus 104 amino acids), has a neutral isoelectric point (7.1 versus 9.1), and only 40% sequence homology with horse heart cytochrome *c*. Figure 1b presents the structure of cytochrome c_2 with the features homologous to horse heart cytochrome *c* color coded as in Figure 1a, based upon structural homology. We have been particularly interested in the so-called hinge region of class I *c*-type cytochromes [9], which is shown in red in both Figure 1a and b. This sequence region, positions 88–102 in *Rhodobacter capsulatus* cytochrome c_2, undergoes a rapid motion in oxidized, but not reduced, *c*-type cytochromes. This motion results in the breaking of the iron-methionyl sulfur bond, and a movement of the hinge away from the heme face, a movement that is sufficiently large that exogenous ligands such as imidazole and pyridine can ligate the iron. The heme face is exposed (open form) ~30 times per s, a rate constant that appears to be conserved throughout evolution. The equilibrium lies strongly on the closed/native side with only ~1% of the molecules in the open form at neutral pH and moderate ionic strength. Interestingly, we have been able to make hinge mutants which can modulate the kinetics of the movement away from the heme face [9]. More recently, we have shown that the hinge kinetics facilitate the dissociation of the oxidized cytochrome from the ferricytochrome c_2-reaction center complex, strongly suggesting that the hinge dynamics play a role in turnover under physiological conditions [10]. Of particular interest is the mutation of lysine 93 to proline (K93P), which results in an increased hinge motion (from ~30 s^{-1} to 700 s^{-1}), presumably as a consequence of the proline ring structure conformationally restricting the peptide backbone in the hinge region which results in weakening the interaction of the hinge with rest of the protein.

In view of the foregoing discussion, we have initiated H/D exchange studies with cytochrome c_2, using proteolytic fragmentation coupled to mass spectrometry. These studies were designed to establish if the domain stability patterns of cytochrome c_2 are the same as those found for cytochrome *c*, and to determine if H/D exchange can facilitate our understanding of the K93P mutation and the resulting dynamic/structural changes in the hinge region.

Materials and Methods

Cytochrome Preparation

Rhodobacter capsulatus wild-type cytochrome c_2 and the K93P mutant were prepared as previously described [11]. Both proteins were concentrated (~1 mM) and stored in 10 mM sodium phosphate and 80 mM KCl (pH 6.8).

Hydrogen Exchange

Hydrogen exchange experiments were initiated by diluting the concentrated cytochrome (~16-fold) into the labeling solution [D_2O and 5 mM sodium phosphate, pD 6.8] to a final concentration of 62.5 μM. Incubation times ranged from 5 s to 24 h. All pH and pD values reported were taken directly from the pH meter and were not corrected for isotopic effects [12]. At each time point, an aliquot of 625 pmol of protein was taken out of the exchange tube and quenched by mixing the solution

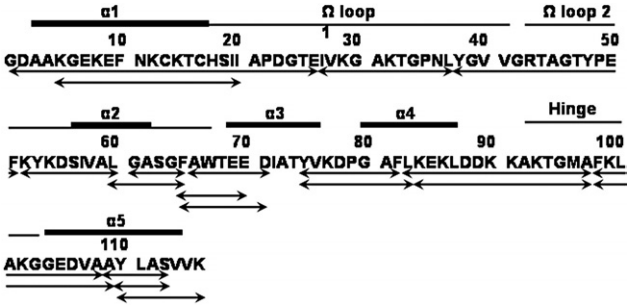

Figure 2. Peptic digestion peptide map for cytochrome c_2 from *Rhodobacter capsulatus*. Each arrow delimits a single peptic peptide. The cytochrome c_2 secondary structure, as determined from the X-ray crystal structure, is shown above the sequence numbering.

in a 1:1 ratio with the quenching buffer [D_2O, 100 mM sodium phosphate, 4 M guanidine deuterium chloride (pD 2.2)]. Oxidized cytochrome was prepared by adding 4-fold molar excess of potassium ferricyanide to the protein stock solution (reduced cytochrome). The labeling solution for experiments with oxidized cytochrome was prepared by addition of potassium ferricyanide to a final concentration of 50 μM.

Hydrogen Exchange Analysis by HPLC-ESI MS

The samples for peptide level analysis were applied to a column of immobilized pepsin packed in house (2 mm * 50 mm, POROS-20AL, Applied Biosystems, Foster City, CA) using water and 0.05% TFA as the mobile phase. The protein digest was collected by a micro-peptide trap (Michom BioResources, Auburn, CA) and washed for 2 min. Peptides in the trap were then eluted from the trap onto a microbore C-18 HPLC column (1 mm * 50 mm, MicroTech Scientific, Vista, CA) coupled to a Finnigan LCQ quadrupole ion trap mass spectrometer (Thermo Electron Corp., Waltham, MA) or Waters Q-TOF II (Milford, MA). Peptides were eluted from the column in 7 min using a gradient of 15 to 45% acetonitrile at a flow rate of 50 μL/min. The micropeptide trap and HPLC column were immersed in ice water during the entire process. The intact protein samples were analyzed similarly to the protein digest, with a couple of exceptions. The pepsin column was not used for the protein, the micro-peptide trap was replaced by a micro-protein trap (Michrom BioResources), and 60% acetonitrile was used for protein elution. Mass spectrometry analyses of all samples within each comparison set were done on the same day with the same instrumental conditions. Deconvolution of intact protein spectra were performed with the program MaxEnt1 (Waters). The error of each data point was determined to be $\pm$2 Da based on multiple measurements. The mass of each peptide was taken as the centroid mass of the isotopic envelope with the program MagTran [13]. The error of each data point was determined to be $\pm$0.2 Da based on multiple measurements.

To account for the exchange of deuterium during the HPLC step (back exchange), and the use of only 16 fold excess deuterium oxide during the labeling step, which limits the forward exchange reaction, an experimental correction is necessary. In our experiments, a 100% deuterated protein control was prepared by diluting the protein stock in the labeling solution and quenching buffer, incubating at 60 °C for 3 h, and then incubating at room-temperature for >24 h. The corrected extent of deuterium incorporation was calculated according to eq 1.

$$m = \frac{m_{\text{exp}} - m_{0\%}}{m_{100\%} - m_{0\%}} * N \quad (1)$$

where m_{exp} is the experimental centroid mass of the peptide at a particular time point, $m_{0\%}$ is the centroid mass of the undeuterated control, $m_{100\%}$ is the centroid mass of the 100% deuterated control, and N is the number of amide hydrogens for the peptide of interest. All data presented here have been corrected for back exchange.

To determine the exchange rates in sub-regions of the peptides, amide hydrogens with similar exchange rates were grouped together within a particular peptide. The overall deuteration level was fit to a general exponential equation $D = N_1\exp(-k_1t) + N_2\exp(-k_2t) + N_3\exp(-k_3t) + N_4\exp(-k_4t)$, where N_1, N_2, N_3 and N_4 represent the number of fast, intermediate, slow, and slowest exchanging amide hydrogens in each peptide, and k_1, k_2, k_3, and k_4 represent their corresponding exchange rate constants [4]. The minimum number of exponential terms to describe the time course was typically 3 to 4. Because of the wide time range studied and the relatively small number of data points, specific rate constants will be reported for only the intermediate and slow exchanging protons. Note however, assuming the exchange of protons in any kinetic regime is an integer; the number of protons exchanging is well defined. The fastest exchanging protons have rate

Table 1. Time course of wild-type, and K93P deuterium exchange[a]

		0% D mass (Da)	Δ m (5 s) Da	Δ m (10 min) Da	Δ m (8 h) Da
Wild-type	Reduced	12,880	26	59	82
	Oxidized		32	64	88
K93P	Reduced	12,894	30	64	93
	Oxidized		36	66	96

[a]The error for each data point was determined to be $\pm$2Da.

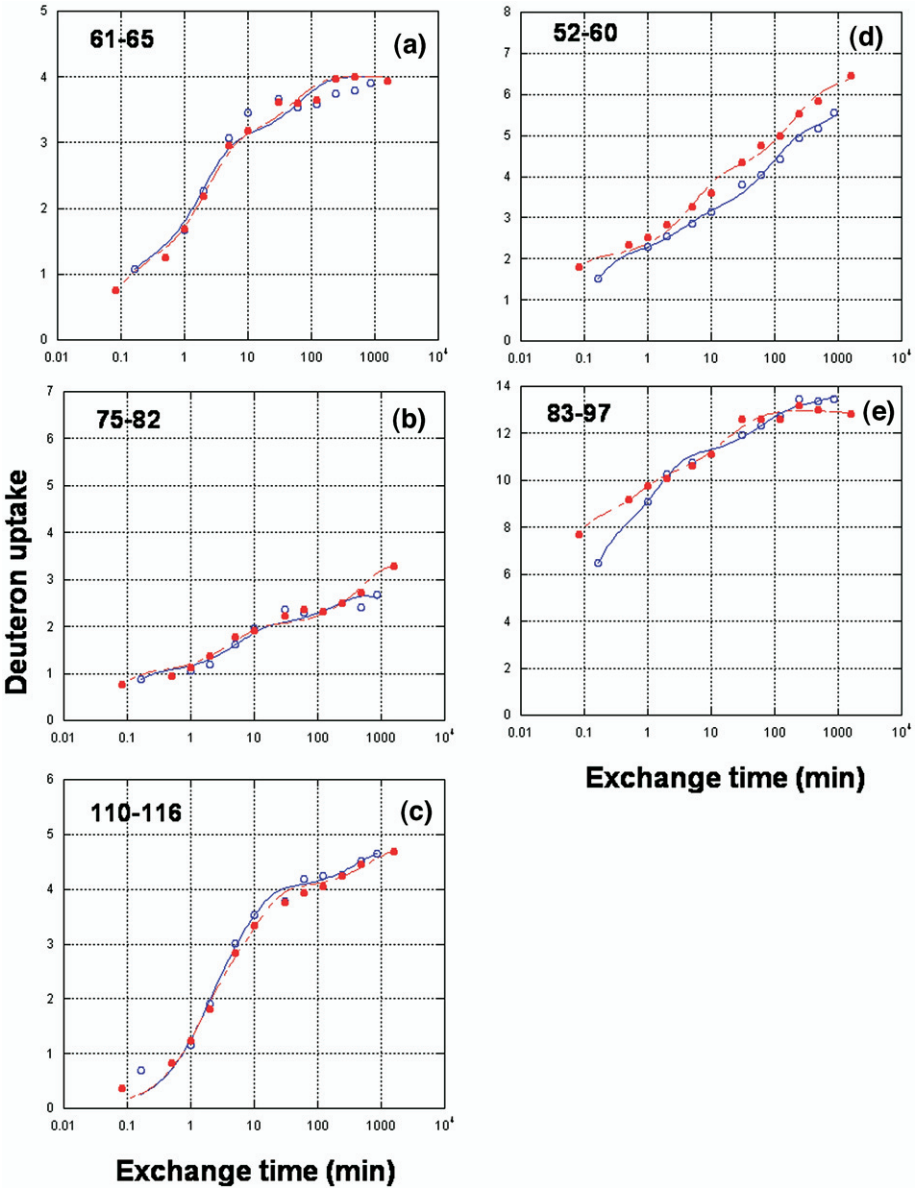

Figure 3. H/D exchange versus semi-log time plots, wild-type cytochrome c_2. Panels (**a**)–(**c**) (peptides 61–65, 75–82, and 110–116, respectively) present typical data for peptides for which exchange kinetics in the two redox states are the same within experimental error. Panels (**d**) and (**e**) (peptides 52–60 and 83–97, respectively) show data for the two peptides for which the oxidized and reduced data significantly differ. Reduced cytochrome data are shown as blue open circles, oxidized cytochrome data are shown as red closed circles. Lines are fits using the general exponential equation as described in Materials and Methods.

constants of >5 min^{-1}, the intermediate, slow, and slowest exchanging protons have rate constants typically in the range of 0.2–1.0 $min^{-1,}$ 0.01–0.05 min^{-1} and <0.001 min^{-1}, respectively. The program Kaleidagraph (Synergy Software, Reading, PA) was used for the nonlinear least-square fit to the kinetic data.

Results

Identification of the Peptides

Unlabeled cytochrome c_2 was digested online by a pepsin column, followed by HPLC separation, and detected by mass spectrometry as described. Nineteen peptides were identified, which cover 97.5% of the sequence (Figure 2). Peptides range from 4 to 26 amino acids. The average peptide size was 11 amino acids.

Exchange Comparison of Intact Wild-Type and K93P in Two Different Oxidation States

The intact protein exchange data are summarized in Table 1. As is obvious from the data, the exchange time course of the oxidized cytochrome c_2 revealed an

Table 2. H/D exchange kinetics, wild-type, and K93P cytochrome c_2

		Reduced/Oxidized Kinetics					
			Intermediate		Slow		
Peptide		Fast (>5 min^{-1}) N/N*	N/N	k(min^{-1})	N/N	k(min^{-1})	Slowest (<0.001 min^{-1}) N/N
52–60	Wild-type	2/2	1/2	0.3/0.2	2/2	0.01/0.01	3/2
	K93P	3/3	0/3	-/0.2	3/2	0.01/0.004	2/0
75–82	Wild-type	1/1	1/1	0.2/0.2	0/1	-/0.003	4/3
	K93P	1/1	1/1	0.3/0.7	1/2	0.03/0.02	3/2
83–97	Wild-type	7/8	4/2	0.7/1.5	2/2	0.02/0.05	1/2
	K93P	11/11	1/1	0.3/0.5	0/0	-/-	1/1

*N/N is the number of protons exchanged in the reduced state/number of protons exchanged in the oxidized state, as determined by the kinetic analysis describes in Materials and Methods.

overall increase in deuteron uptake relative to the reduced cytochrome, consistent with destabilization in the oxidized relative to the reduced state. This is in agreement with a previous H/D exchange NMR study [14], as well as H/D exchange studies on a related protein, horse heart cytochrome *c* [5]. Exchange data of the mutant K93P also revealed an overall destabilization compared to wild-type, in both redox states, as well as a destabilization of oxidized K93P relative to its reduced state. This result is consistent with the previously reported ~28% destabilization of oxidized K93P relative to oxidized wild-type, based on guanidine titrations measured at 220 nm using circular dichroism [9].

Exchange Kinetics, Wild-Type Cytochrome$_2$

Among the peptides identified, 10 nonoverlapping peptides were selected for analysis. For the wild-type, a comparison of the deuterium levels found in these peptides as a function of time divided the peptides into two groups. The first group consisting of peptides, 1–26, 27–37, 38–51, 61–65, 66–71, 75–82, 98–109, and 110–116, show similar or identical exchange kinetics between cytochrome c_2 redox states. Three examples are shown in Figure 3a, b, and c). In contrast, two peptides, 52–60 and 83–97, showed distinctly different time-dependent exchange behaviors in the two redox states (Figure 3d and e). As can be seen in Figure 1b, these two regions encompass a portion of the hinge region (88–97, 10 amide hydrogens) and a portion of Ω loop 2 (52–55, 3 amide hydrogens). As can be seen from Figure 3d, and the summary data in Table 2, for peptide 52–60, there is an increase in the number of protons exchanging with intermediate kinetics and a decrease of protons exchanging in the slowest kinetic regime in the oxidized state as compared to the reduced state. This is consistent with decreased stability of Ω loop 2 in the oxidized form. In the case of peptide 83–97, there are significant increases in both the kinetics and number of protons exchanging in the oxidized cytochrome, a consequence of the hinge region becoming destabilized in the oxidized state.

Exchange Kinetics, K93P

Comparing the exchange kinetics for the two K93P redox states yields generally similar conclusions as those found for the wild-type cytochrome, that is, no significant effect of redox state on eight peptides (data not shown), but a significant increase in the exchange kinetics for peptides 52–60 and 83–97 for the oxidized mutant as compared to the reduced form (data not shown). Comparing wild-type and K93P and the corresponding redox states, we find that seven peptides have essentially identical exchange kinetics (data not shown). In contrast, three peptides have significantly different exchange kinetics. Figure 4a, b, and c and Table 2 compare the exchange kinetics for peptides 52–60, 75–82, and 83–97 for reduced wild-type and K93P. In the case of peptide 52–60, there appears to be a general destabilization apparently involving both the helix-2 and Ω loop amide protons. However, in the case of peptide 75–82 (the C-terminus of helix-3, a short intervening region, and the N-terminus of helix-4) the principal effect is on the slow and slowest exchanging protons (Table 2). This suggests the destabilization of a portion of at least one of the two helix elements on mutation, presumably involving slow or slowest exchange protons. Finally, in the case of peptide 83–97, the mutation results in a significant increase in the exchange kinetics of the three fastest exchange regions as compared to the wild-type cytochrome. The comparison of the oxidized wild-type and K93P yields a similar pattern to that of the reduced state, with the same three peptides exchanging more rapidly in the mutant cytochrome (Figure 4d, e, and f). Note that in the case of peptide 83–97 there are only 13 exchangeable amide protons in the proline mutant as compared to 14 in the wild-type cytochrome.

Discussion

For wild-type cytochrome c_2, and Class I *c*-type cytochromes in general, it is well established that the oxidized state is significantly destabilized relative to the reduced state, a consequence in part of burying a formal

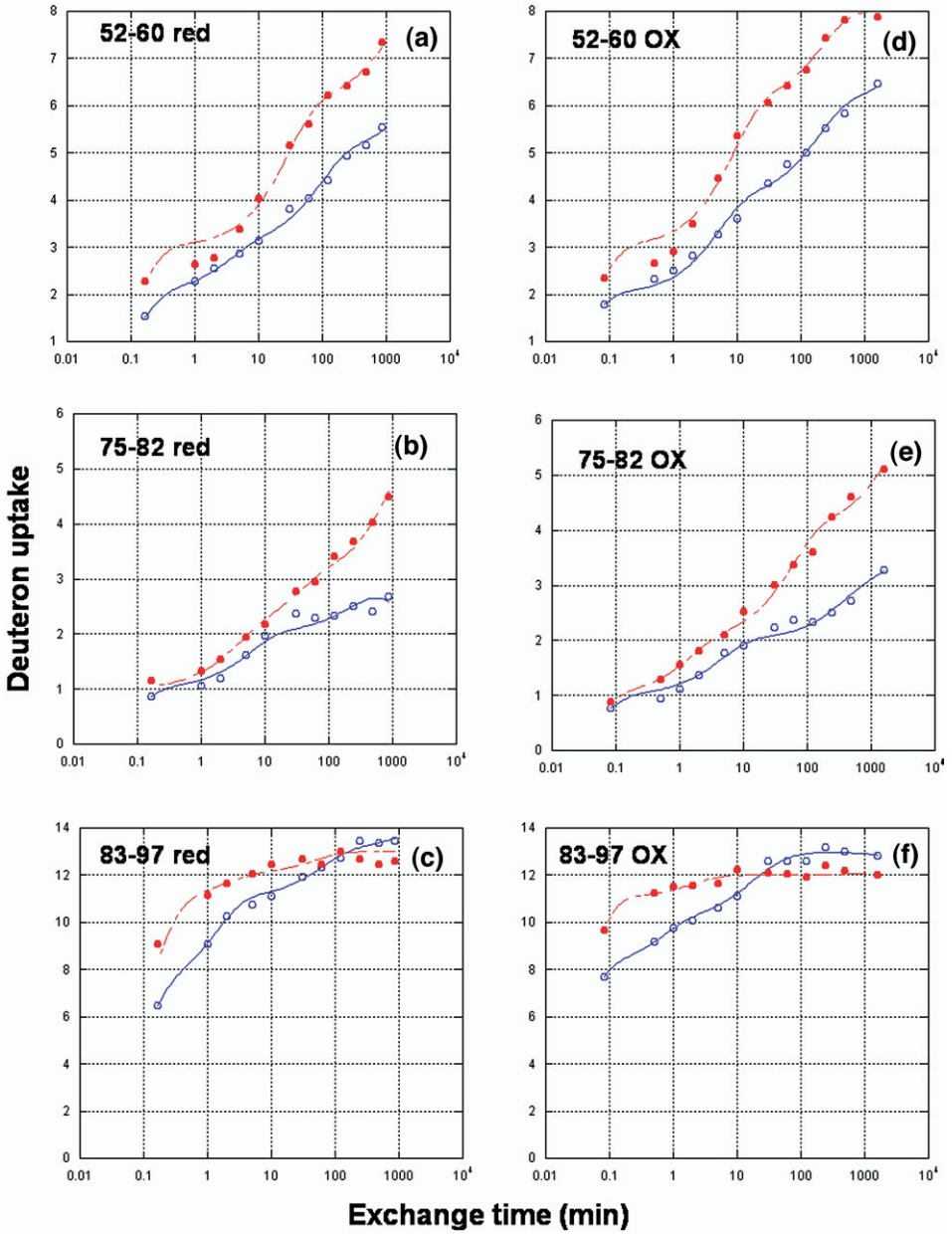

Figure 4. Comparison of wild-type and K93P cytochrome c_2 peptides with significant differences in H/D exchange. Panels (**a**)–(**c**) are peptides 52–60, 75–82, and 83–97, respectively, for reduced cytochrome c_2 (blue open circle) and reduced K93P (red closed circle). Panels (**d**)–(**f**) are peptides 52–60, 75–82, and 83–97, respectively, for oxidized cytochrome c_2 (blue open circle) and oxidized K93P (red closed circle). Lines are fits using the general exponential equation as described in Materials and Methods.

charge of plus one (due to the ferric heme iron) in the hydrophobic protein interior [15]. Moreover, it is also clear that the hinge region is significantly destabilized on oxidation with a corresponding increase in its dynamics [9]. Indeed, we find that two peptides have enhanced exchange kinetics in the oxidized state as compared to the reduced state and one of these peptides (83–97) covers much of the hinge region. Englander and coworkers [3], using exchange studies, have proposed five "foldons", which reflect the folding units in the horse cytochrome *c* structure. These are summarized in Table 3, and using amino acid sequence and structural homology, correlated with cytochrome c_2. The relative stabilities of the five foldons are N yellow Ω loop < red unit < outer yellow neck < green unit < blue unit in horse heart cytochrome *c* [3], which is consistent with cytochrome c_2 peptides 52–60 covering a portion of the N yellow Ω loop, and the hinge region (83–97, red unit) being the least stable. Our results are also consistent with the H/D exchange measurements reported previously using mass spectrometry to compare the two redox states of horse

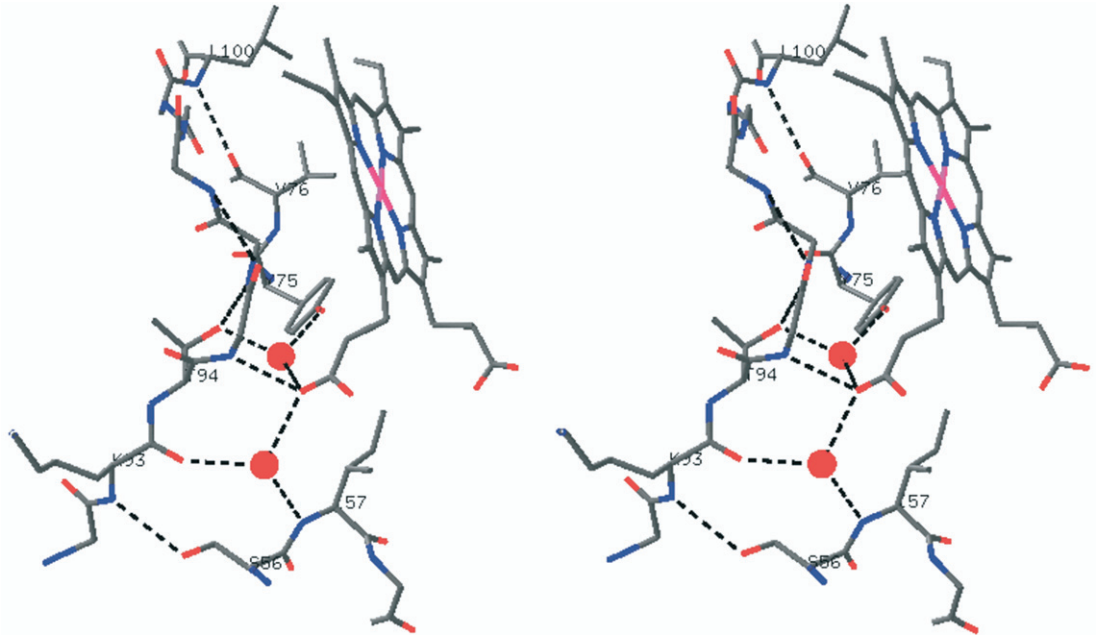

Figure 5. Stereo view of Hydrogen bonding interactions between hinge region and Ω loop 2 in wild-type cytochrome c_2. Colored coding is standard CPK, with the bound waters in red.

cytochrome *c* [5]. That is, cytochrome c_2 peptides 52–60 (counterpart of the N yellow Ω loop in horse) and peptide 83–97 (counterpart of the hinge in horse) exchange much more readily in the oxidized state, as in the case of horse heart. However, in the case of cytochrome c_2 the bulk of peptides encompassing the two Ω loops (positions 28–54), that is, peptides 27–37 and 38–51, are not measurably destabilized in the oxidized state. This is in sharp contrast to the horse cytochrome *c* H/D exchange studies [5] where there is significant destabilization in the Ω loop on oxidation. Presumably, this results from the fact that in cytochrome c_2 the Ω loop is stabilized by the presence of two short regions of β-sheet (positions 19–21 with 25–27 and positions 43–45 with 65–67), in contrast to only one such region in horse cytochrome *c*. Thus H/D exchange as determined by mass spectrometry, in spite of being a relatively low-resolution technique, has in the case of cytochrome c_2 resolved relatively subtle structural features.

Table 3. Horse and *Rb. capsulatus* cytochrome *c* homologous regions and foldons[a]

Amino Acid Sequence Position		Structural feature	Nomenclature
cyto. c_2	cyto. *c*		
3–14	3–12	α-helix 1	Blue unit
19–21	NA	β-sheet 1[b]	NA
25–27	NA	β-sheet 1	NA
28–35	20–36	Ω-loop 1	Green unit
43–45	37–39	β-sheet 2	Outer yellow neck
46–54	40–57	Ω-loop 2	N-yellow loop
56–62	50–54	α-helix 2	In N-yellow loop
65–67	58–61	β-sheet 2	Outer yellow neck
69–76	61–68	α-helix 3	Green unit
80–87	72–74	α-helix 4	NA
88–102	71–85	Hinge	Red Unit
104–114	88–102	α-helix 5	Blue Unit

[a]Secondary structure as assigned by Swiss-Prot Deep View
[b]Cyto. c_2 has two small regions of β-sheet (β-sheet 1 and 2), cyto. *c* has only one (β-sheet 2)

The destabilization of regions containing peptides 83–97 and 52–60 appears to be linked. This results from an extensive hydrogen bond network between these two regions as shown in Figure 5. These interactions include hydrogen bonds from the backbone amide hydrogen of K93 to the S56 hydroxyl side-chain, and an indirect hydrogen bond from the backbone amide hydrogen of I57 to the K93 carbonyl oxygen through a bound water molecule, which is also hydrogen bonded to one of the heme propionates. Presumably, when the hinge region is destabilized on oxidation of the heme iron, the destabilization is propagated to a portion of peptide 52–60, altering its exchange kinetics.

The K93P mutation has two particularly dramatic effects on the properties of the cytochrome c_2. First, it leads to a substantial destabilization of the protein relative to the wild-type cytochrome, and second, results in a substantial increase in the hinge dynamics (~ 20-fold) [9]. Upon K93P mutation, the H/D exchange kinetics of three regions are significantly changed relative to the wild-type protein. These include peptides 52–60, 75–82, and 83–97. Note that these three peptides are affected in both redox states, and are the only peptides affected for the time range studied. This strongly suggests that the three pep-

tides (and their corresponding domains) form a cooperative structural unit whose disruption results in destabilization of the cytochrome. Interestingly, peptides 52–60 and 83–97 are those that are most affected by oxidation in the wild-type cytochrome, with their structural relation described above and shown in Figure 5. Presumably the mutation destabilizes the 52–60 and 83–97 regions in both redox states, by amplifying the destabilization observed in the oxidized state, that is, by structurally altering the interaction between the N-terminus of the hinge and the cytochrome c_2 Ω 2 loop which in turn weakens the iron-methionyl sulfur bond. This is consistent with the substantially increased hinge kinetics (30 s^{-1} goes to 700 s^{-1}) in the oxidized state [9] and a destabilization in the reduced state. The destabilization of peptide 75-82 in the K93P mutant supports the interpretation provided here, since it suggests that interaction of the Y75 hydroxyl, which is hydrogen bonded to bound water in the wild-type cytochrome (Figure 5), is weakened. This water is also hydrogen bonded to the T94 hydroxyl and the front heme propionate. Apparently, the change in oxidation state with wild-type cytochrome is not sufficient to disturb this interaction, but the mutation at K93 does.

In summary, the H/D exchange studies reported here allow us to draw conclusions not readily determined by other approaches. For example, the two redox states of *Rhodobacter capsulatus* cytochrome c_2 have been studied by H/D exchange using NMR [14], however the data reported for exchange was limited, with the earliest time 50 min, and the major differences in the slowest exchanging protons at very long times (>20 h). We find, not unexpectedly, that the relative stability of cytochrome c_2 domains are generally consistent with the horse cytochrome *c* H/D exchange studies. We can show, however, that the second short β-sheet suggested by the cytochrome c_2 crystal structure exists in solution and stabilizes the Ω 2 loop. Thus, H/D exchange data are able to detect relatively subtle structural differences between the two homologous, but not identical, cytochromes. Moreover, oxidation and thus changing the formal charge on the heme iron to plus one, destabilizes the hinge region (expected) and this destabilization is propagated to the Ω 2 loop through altering/modifying hydrogen bond interactions. Finally, apparently the K93P mutation alters the hinge dynamics in the oxidized state, and destabilizes the hinge in the reduced protein, in part by amplifying the effect of oxidation by disrupting a more extensive hydrogen bond network involving the Y75 hydroxyl, a bound water, the front propionate and the T94 hydroxyl, as well as interaction between the N-terminus of the hinge peptide and residues 56 and 57 in Ω loop 2.

Acknowledgments

This work was financially supported by the NIH grant GM21277 to MAC, grant GM051387 to VHW, and the 2005–2006 Pfizer Graduate Research Fellowship in Analytical Chemistry to GC.

References

1. Bai, Y.; Sosnick, T. R.; Mayne, L.; Englander, S. W. Protein folding intermediates: Native-state hydrogen exchange. *Science* **1995,** *269*(5221), 192–197.
2. Hoang, L.; Maity, H.; Krishna, M. M. G.; Lin, Y.; Englander, S. W. Folding units govern the cytochrome *c* alkaline transition. *J. Mol. Biol.* **2003,** *331*(1), 37–43.
3. Krishna Mallela, M. G.; Lin, Y.; Mayne, L.; Englander, S. W. Intimate view of a kinetic protein folding intermediate: residue-resolved structure, interactions, stability, folding, and unfolding rates, homogeneity. *J. Mol. Biol.* **2003,** *334*(3), 501–513.
4. Zhang, Z.; Smith, D. L. Determination of amide hydrogen exchange by mass spectrometry: A new tool for protein structure elucidation. *Protein Sci.* **1993,** *2*(4), 522–531.
5. Dharmasiri, K.; Smith, D. L. Regional stability changes in oxidized and reduced cytochrome *c* located by hydrogen exchange and mass spectrometry. *J. Am. Soc. Mass Spectrom.* **1997,** *8*(10), 1039–1045.
6. Englander, J. J.; Del Mar, C.; Li, W.; Englander, S. W.; Kim, J. S.; Stranz, D. D.; Hamuro, Y.; Woods, V. L., Jr. Protein structure change studied by hydrogen-deuterium exchange, functional labeling, and mass spectrometry. *Proc. Natl. Acad. Sci. U.S.A.* **2003,** *100*(12), 7057–7062.
7. Benning, M. M.; Wesenberg, G.; Caffrey, M. S.; Bartsch, R. G.; Meyer, T. E.; Cusanovich, M. A.; Rayment, I.; Holden, H. M. Molecular structure of cytochrome c_2 isolated from *Rhodobacter capsulatus* determined at 2.5. ANG. resolution. *J. Mol. Biol.* **1991,** *220*(3), 673–685.
8. Meyer, T. E.; Cusanovich, M. A. Discovery and characterization of electron transfer proteins in the photosynthetic bacteria. *Photosynth. Res.* **2003**, *76*(1/3), 111–126.
9. Dumortier, C.; Fitch, J.; Van Petegem, F.; Vermeulen, W.; Meyer, T. E.; Van Beeumen, J. J.; Cusanovich, M. A. Protein dynamics in the region of the sixth ligand methionine revealed by studies of imidazole binding to *Rhodobacter capsulatus* cytochrome c_2 hinge mutants. *Biochemistry* **2004,** *43*(24), 7717–7724.
10. Devanathan, S.; Salamon, Z.; Tollin, G.; Fitch, J.; Meyer, T. E.; Cusanovich, M. A. Binding of oxidized and reduced cytochrome c_2 to photosynthetic reaction centers: Plasmon-waveguide resonance spectroscopy. *Biochemistry* **2004,** *43*(51), 16405–16415.
11. Caffrey, M. S.; Cusanovich, M. A. Site-specific mutagenesis studies of cytochromes *c*. *Biochim. Biophys. Acta* **1994,** *1187*(3), 277–288.
12. Englander, J. J.; Rogero, J. R.; Englander, S. W. Protein hydrogen exchange studied by the fragment separation method. *Anal. Biochem.* **1985,** *147*(1), 234–244.
13. Zhang, Z.; Marshall, A. G. A universal algorithm for fast and automated charge state deconvolution of electrospray mass-to-charge ratio spectra. *J. Am. Soc. Mass Spectrom.* **1998,** *9*(3), 225–233.
14. Zhao, D.; Hutton, H. M.; Gooley, P. R.; MacKenzie, N. E.; Cusanovich, M. A. Redox-related conformational changes in *Rhodobacter capsulatus* cytochrome c_2. *Protein Sci.* **2000,** *9*(9), 1828–1837.
15. Blouin, C.; Wallace, C. J. A. Protein matrix and dielectric effect in cytochrome *c*. *J. Biol. Chem.* **2001,** *276*(31), 28814–28818.